CRYSTAL GROWTH & DESIGN

ARTICLE

pubs.acs.org/crystal

Neutral and Zwitterionic Polymorphs of 2-(*p*-Tolylamino)nicotinic Acid

Naba K. Nath, S. Sudalai Kumar, and Ashwini Nangia*

School of Chemistry, University of Hyderabad, Central University PO, Prof. C. R. Rao Road, Gachibowli, Hyderabad 500 046, India

Supporting Information

ABSTRACT:

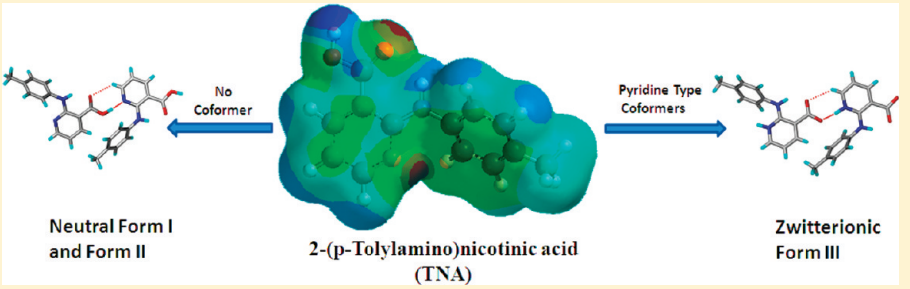

2-(*p*-Tolylamino)nicotinic acid (TNA) was crystallized in three polymorphic forms. The crystal structures of forms I and II are sustained by the neutral O−H···N hydrogen bond from the COOH donor to the pyridine N acceptor, whereas proton transfer occurred in form III to give a zwitterionic structure of $N-H^{+}\cdots O^{-}$ hydrogen bond. Form III could be obtained only in the presence of pyridine-type coformers. The trimorphs were characterized by IR, Raman, and ss-NMR spectroscopy, DSC, and single crystal X-ray diffraction. The neutral form I and zwitterionic form III are 2D isostructural, whereas form II has a different crystal packing and molecular conformation. XPac analysis showed the 2D supramolecular construct and similarity in crystal structures of forms I and III. The difference in hydrogen bonding between the neutral and zwitterionic polymorph is analyzed by Hirshfeld surfaces. The isolation of zwitterionic TNA as a complex with *m*-nitrobenzoic acid and a TNA salt with *o*-aminopyridine provides a mechanistic rationale for the crystallization of the rare zwitterionic structure of amphoteric TNA molecule.

INTRODUCTION

Ampholites are amphoteric compounds that contain both acidic and basic functional groups, and such molecules can exist as zwitterions in certain pH ranges. Zwitterions contain both positive and negative charges on different atoms of the same molecule, but they are electrically neutral through a net cancellation of the positive and negative charge.[1] Amino acids are the commonest example of a zwitterion. Some other zwitterionic categories are buffers, detergents, dyes, and drugs. Amphoteric compounds are frequently encountered as drugs in medicinal chemistry and drug metabolites in biochemistry. Amphoteric drug molecules predominantly exist as charged species in the physiological pH range and are therefore able to bind to the plasma targets in the body.[2] The variation of pH in the stomach and digestive tract (1.2−6.8)[3] can cause changes in the physicochemical properties of neutral/zwitterionic drugs, such as solubility, stability, and permeability.

RESULTS AND DISCUSSION

Background. There are very few molecules that exhibit both neutral and zwitterionic crystal structures in the Cambridge Structural Database[4] (CSD ver 5.32, November 2010, May 2011 update) (Scheme 1). We were able to extract only four polymorphic sets of neutral and zwitterionic forms among solved X-ray crystal structures of single-component organic molecules archived in the CSD. Clonixin[5] form II (BIXGIY04) is zwitterionic, whereas the other polymorphs of this tetramorphic compound are neutral (BIXGIY01, BIXGIY02, BIXGIY03). The monoclinic polymorph of norfloxacin[6] is zwitterionic (VETVOG01), whereas the triclinic structure is neutral (VETVOG). Anthranilic acid[7] is trimorphic: neutral monoclinic (AMBACO08), neutral orthorhombic (AMBACO05), and zwitterionic orthorhombic (AMBACO07). Torasemide[8] has a crystal structure containing one zwitterion and one neutral molecule (TORSEM02), whereas the second polymorph is completely zwitterionic (TORSEM04).

Many diarylamines are anti-inflammatory,[9] e.g., niflumic acid, clonixin, mefenamic acid, tolfenamic acid, flufenamic acid meclofenamic acid, and diclofenac. Several of these molecules exhibit polymorphism.[10] However, except clonixin,[5] none of these compounds, including the recently reported pentamorphs of tolfenamic acid,[10e] fall in the category of zwitterion and neutral polymorphic structures. Torasemide and anthranilic acid have

Received: July 7, 2011
Revised: August 17, 2011
Published: August 29, 2011

Scheme 1. Molecules Exhibiting Zwitterionic and Neutral Polymorphs Extracted from the CSD

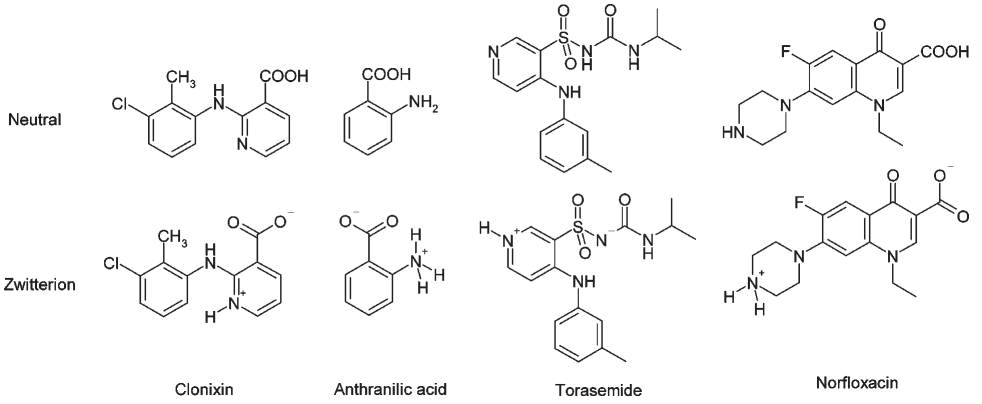

Scheme 2. Molecular Structure of 2-(*p*-Tolylamino)nicotinic Acid (TNA)

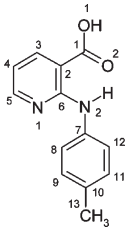

Scheme 3. Diarylamine Carboxylic Acids Recently Reported by Li's Group[11]

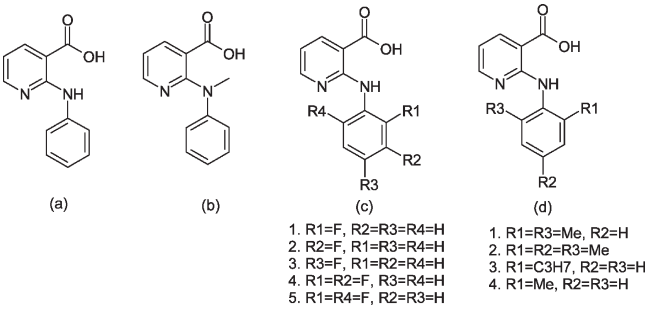

both neutral and zwitterionic molecules in the same crystal structure. We studied the crystal structures of 2-(*p*-tolylamino)-nicotinic acid (TNA) (Scheme 2) in the above background to explore neutral/zwitterion polymorphic behavior. Li[11] and co-workers recently reported polymorphism in some diarylamine carboxylic acids. Even though these molecules (Scheme 3) are structurally very similar to TNA, the authors did not disclose any example of neutral and zwitterionic polymorph sets in their studies. Both 2-(phenylamino)nicotinic acid and 2-[methyl-(phenyl)amino]nicotinic acid (molecules a and b) were found to be tetramorphic in their polymorph hunt.

Our recent studies on synthon competition and cooperation in cocrystals of carboxylic acids and pyridines suggested that it is very difficult to predict the status of proton migration based on pK_a values of carboxylic acid and pyridine, especially when extra functional groups such as amine and hydroxyl are present.[12] The utility of the ΔpK_a rule, i.e., proton transfer will occur when the difference in pK_a between the conjugate acid of the base and the carboxylic acid is >3 and a neutral state will occur when $\Delta pK_a < 3$, is widely accepted in the pharmaceutical literature.[13] In our experience, the neutral and the ionic states can be reliably predicted when $\Delta pK_a < 0$ and $\Delta pK_a > 3$, respectively, but the range $0 < \Delta pK_a < 3$ is somewhat of a gray zone, wherein it is difficult to know the answer beforehand. Incidentally (phenylamino) nicotinic acids fall in the gray zone category: the pK_a of the conjugate acid of pyridine is ~5.3, secondary ammonium is ~10.7, and carboxylic acid is ~4.2.[14] Despite the high basicity of the secondary amine, its proton-accepting strength is lowered in the molecules under study because of adjacent electron-withdrawing pyridine and carboxylic acid groups, with the result that the more basic functional group in such molecules is the pyridine moiety. The calculated pK_a values for clonixin are 1.69 and 4.80, which are comparable to those for the closely related niflumic acid (1.70 and 4.71).[13b] We therefore felt that crystallization under different conditions of solvent, concentration, temperature, additives, coformers, etc. is a logical way to explore this system for polymorphism. The conformational flexibility of the molecule could make it polymorph promiscuous.[15] The ampholitic nature of the molecule meant that there was likelihood of obtaining neutral and zwitterionic polymorphs in the supramolecular solid-state form space by exhaustive exploration of experimental conditions. Polymorph screening of TNA was performed using different crystallization techniques including cocrystallization with carboxylic acid and pyridine derivatives as coformers.

TNA Polymorphs. We report zwitterionic and neutral crystal structures of TNA polymorphs. Forms I and II are sustained by the neutral O—H···N hydrogen bond, whereas form III has a zwitterionic molecule and N—H^+···O^- hydrogen bond. Interestingly, the zwitterionic structure of TNA could be crystallized only in cocrystallization experiments when a stoichiometric amount of *o*-bromo-*m*-hydroxypyridine, *o*-aminopyridine, isonicotinic acid, or nicotinic acid was added as a coformer in separate experiments. We also report a cocrystal of TNA with *m*-nitrobenzoic acid and a salt of *o*-aminopyridine to understand the formation of zwitterionic polymorph under the attempted cocrystallization conditions

TNA was crystallized (preparation is reported in the Experimental Section) by using different techniques, such as solvent

dx.doi.org/10.1021/cg200853u |*Cryst. Growth Des.* 2011, 11, 4594–4605

Table 1. Crystallographic Parameters of TNA Polymorphs and Cocrystals

TNA	form I	form II	form III	form III	$NH^+-TNA-COO^-\cdot 2NBA$	$AP-NH^+\cdot TNA-COO^-$
empirical formula	$C_{13}H_{12}N_2O_2$	$C_{13}H_{12}N_2O_2$	$C_{13}H_{12}N_2O_2$	$C_{13}H_{12}N_2O_2$	$C_{27}H_{22}N_4O_{10}$	$C_{18}H_{18}N_4O_2$
formula weight	228.25	228.25	228.25	228.25	562.49	322.36
crystal system	monoclinic	orthorhombic	orthorhombic	orthorhombic	triclinic	orthorhombic
space group	$P2_1/n$	*Pbca*	*Pbca*	*Pbca*	$P\bar{1}$	$P2_12_12_1$
T (K)	100	100	100	298	298	298
a/Å	11.038(10)	14.2565(16)	9.0787(11)	9.250(4)	7.8000(8)	6.8022(8)
b/Å	9.067(8)	10.7542(15)	14.2261(17)	14.207(4)	13.0415(16)	10.4120(12)
c/Å	11.392(10)	14.769(3)	17.154(2)	17.509(10)	14.0098(15)	23.206(3)
α/deg	90	90	90	90	64.870(11)	90
β/deg	101.860(14)	90	90	90	86.132(9)	90
γ/deg	90	90	90	90	85.992(9)	90
V/Å^3	1115.8(17)	2264.3(6)	2215.6(5)	2301.1(17)	1286.0(3)	1643.6(3)
D_{calcd} (g cm^{-3})	1.359	1.339	1.369	1.318	1.453	1.303
μ (mm^{-1})	0.094	0. 092	0.094	0.091	0.113	0.088
Z/Z'	4/1	8/1	8/1	8/1	2/1	4/1
reflns collected	10196	10798	20081	5988	9618	15003
unique reflns	2190	4319	2160	2097	5273	3220
observed reflns	1987	2306	2005	866	3625	3101
R_1 [$I > 2\sigma(I)$]	0.0598	0.0497	0.0521	0.0646	0.0399	0.0420
wR_2 (all)	0.1827	0.1026	0.1475	0.1350	0.1033	0.0928
goodness-of-fit	1.188	0.872	1.185	0.929	1.039	1.162
diffractometer	SMART APEX CCD	Xcalibur Gemini Eos CCD	SMART APEX CCD	Xcalibur Gemini Eos CCD	Xcalibur Gemini Eos CCD	SMART APEX CCD

evaporation, melting, sublimation, slow cooling, flash cooling, and crystallization in the presence of different coformers. Three polymorphs were crystallized in these manual screen experiments. Forms I and II crystallized concomitantly from several solvents, such as acetone, methanol, ethanol, ethyl acetate, acetonitrile, chloroform, and THF. Form II was obtained exclusively by melt crystallization and pure form I was crystallized from acetone. The polymorph identity was established after each experiment by powder X-ray diffraction. Zwitterionic form III was obtained when TNA was cocrystallized with *o*-bromo-*m*-hydroxypyridine, *o*-aminopyridine, isonicotinic acid, or nicotinic acid in CH_3CN solvent. The experimental conditions could not be fully optimized even after our best efforts; occasionally these cocrystallizations also gave form I or II or a salt of TNA with *o*-aminopyridine. The particular crystalline form(s) in any batch were checked by determining the unit cell of a few single crystals. The presence of the coformer was however important: form III could not be crystallized from solution crystallization in the absence of pyridine functional group containing coformers. Cocrystallization of TNA and *o*-aminopyridine (AP) in CH_3CN resulted in the corresponding salt ($AP-NH^+\cdot TNA-COO^-$) along with forms III and I/II occurring concomitantly. Cocrystallization of TNA with *m*-nitrobenzoic acid (NBA) resulted in 1:2 stoichiometry of the components, wherein TNA was in its zwitterionic state and the cofomer was neutral ($NH^+-TNA-COO^-\cdot 2NBA$). The structures of all new compounds were characterized by single crystal X-ray diffraction (Table 1).

Crystal Structure Analysis. Block morphology crystals of form I were obtained from acetone and the reflections data were solved and refined in the monoclinic space group $P2_1/n$ with one molecule in the asymmetric unit. Chains of molecules linked by acid−pyridine two point synthon (O1−H1···N1, 1.59 Å, 175.6° and C5−H5···O2, 2.55 Å, 133.1°) are connected by C−H···π interaction (C4−H4···C12, 2.88 Å, 145.8°) to make a sheet structure, and such sheets are connected by C−H···O (C12−H12···O1, 2.58 Å, 174.7°) and C−H···π interactions (C9−H9···C3, 2.84 Å, 162.1°) (Figure 1). Hydrogen bonds are listed in Table 2.

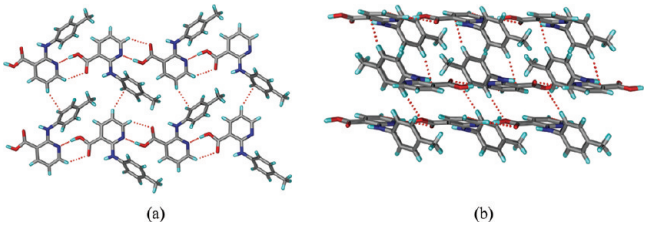

Figure 1. (a) Chains of molecules sustained by the acid−pyridine synthon are connected by C−H···π interaction to make a 2D sheet in the crystal structure of form I. (b) C−H···O and C−H···π interactions in the interlayer region.

Block morphology crystals of form II obtained from methanol were solved and refined in the orthorhombic space group *Pbca* ($Z' = 1$). The acid−pyridine synthon (O1−H1···N1, 1.68 Å, 174.7° and C5−H5···O2, 2.49 Å, 136.1°) connects the molecular chains, and additional C−H···O interaction (C13−H13A···O2, 2.59 Å, 150.4°) assemble the zigzag sheet structure. There is offset $\pi\cdots\pi$ stacking (3.39 Å) between the pyridyl rings (Figure 2).

Block morphology crystals of form III were obtained in attempted cocrystallization with *o*-aminopyridine in acetonitrile solvent. The crystal structure was solved and refined in the orthorhombic space group *Pbca*. The X-ray crystal structure and difference electron density maps (100 K data set)

dx.doi.org/10.1021/cg200853u |*Cryst. Growth Des.* 2011, 11, 4594–4605

Table 2. Hydrogen Bonds in Crystal Structures of TNA

interactions	H···A/Å	D···A/Å	∠D−H···A/deg	symmetry code
		TNA Form I		
N2−H2···O2	1.90	2.591(4)	147.3	intramolecular
O1−H1···N1	1.59	2.591(4)	175.6	$1/2 + x, 1/2 - y, 1/2 + z$
C3−H3···O1	2.34	2.672(5)	99.8	intramolecular
C5 −H5···O2	2.55	3.272(5)	133.1	$-1/2 + x, 1/2- y, -1/2 + z$
C12−H12···O1	2.58	3.526(5)	174.7	$3/2 - x, -1/2 + y, 1/2 - z$
		TNA Form II		
O1−H1···N1	1.68	2.663(1)	174.7	$-1/2 + x, 1/2 - y, 1 - z$
N2−H2···O2	1.94	2.669(1)	141.7	intramolecular
C3−H3···O1	2.38	2.704(2)	100.2	intramolecular
C5−H5···O2	2.49	3.222(2)	136.1	$1/2 + x, 1/2 - y, 1 - z$
C13−H13A···O2	2.58	3.452(2)	150.4	$1/2 + x, y, 1/2 - z$
		TNA Form III at 100 K		
N1−H1···O1	1.59	2.579(2)	141.6	$3/2 - x, 1/2 + y, z$
N2−H2···O2	1.84	2.630(2)	144.1	intramolecular
C3−H3···O1	2.39	2.722(3)	100.0	intramolecular
C5−H5···O2	2.55	3.312(3)	137.0	$3/2 - x, 1/2 + y, z$
C9−H9···O2	2.46	3.379(3)	164.0	$1 - x, 1/2 + y, 1/2 - z$
C12−H12···O1	2.52	3.463(3)	172.4	$-1/2 + x, 1/2 - y, -z$
		TNA Form III at 298 K		
N1−H1···O1	1.28	2.571(4)	164.2	$3/2 - x, -1/2 + y, z$
N2−H2···O2	1.91	2.644(4)	137.4	intramolecular
C3−H3···O1	2.38	2.716(4)	101.0	intramolecular
C5−H5···O2	2.52	3.273(4)	137.7	$3/2 - x, -1/2 + y, z$
C9−H9···O2	2.57	3.485(6)	166.5	$1 - x, -1/2 + y, 1/2 - z$
		NH^+−TNA−COO^-·2NBA		
N1−H1···O6	2.17	2.962(2)	152.5	x, y, z
N2−H2···O2	1.91	2.621(2)	139.1	intramolecular
N2−H2···O7	2.49	3.176(2)	137.2	$2 - x, -y, 1 - z$
O3−H3A···O1	1.66	2.568(2)	170.1	$-1 + x, y, -1 + z$
O3−H3···O2	2.58	3.056(2)	112.7	$-1 + x, y, -1 + z$
O8−H8A···O2	1.63	2.600(2)	170.4	$2 - x, -y, 1 - z$
C3−H3···O1	2.44	2.763(2)	100.3	intramolecular
C5−H5···O5	2.53	3.286(2)	138.8	x, y, z
C5−H5···O10	2.33	3.041(2)	132.5	$1 - x, 1 - y, -z$
C8−H8···O1	2.40	3.316(2)	168.2	$2 - x, 1 - y, 1 - z$
C12−H12···O9	2.53	3.447(2)	167.5	$x, y, 1 + z$
C19−H19···O9	2.51	3.354(3)	151.9	$1 - x, -y, -z$
C25−H25···O5	2.50	3.431(2)	177.0	$1 - x, 1 - y, -z$
C26−H26···O4	2.53	3.457(2)	174.0	$1 - x, 1 - y, -z$
		AP−NH^+·TNA−COO^-		
N2−H2···O2	1.85	2.626(2)	146.2	intramolecular
N3−H3A··· O1	1.92	2.806(2)	169.5	$1/2 + x, 3/2 - y, 2 - z$
N3−H3B···O1	1.94	2.843(2)	176.2	$1 + x, y, z$
N4−H4A···O2	1.74	2.657(2)	177.2	$1 + x, y, z$
C8− H8···N1	2.3217	2.919(2)	121.7	intramolecular

showed that the carboxylic acid proton had migrated to the pyridine N and that proton transfer was complete to give a zwitterion. When reflections on the same crystal were collected at room temperature (298 K), only partial proton transfer was observed. There was no bulk phase transition between 100 and 300 K other than the slight hydrogen atom shift.

The carboxylate−pyridinium heterosynthon via N^+−H···O^- hydrogen bond ($N1^+$−H1···$O1^-$, 1.59 Å, 170.9°) and auxiliary C−H···O hydrogen bond (C5−H5···O2, 2.55 Å,

dx.doi.org/10.1021/cg200853u |*Cryst. Growth Des.* 2011, 11, 4594–4605

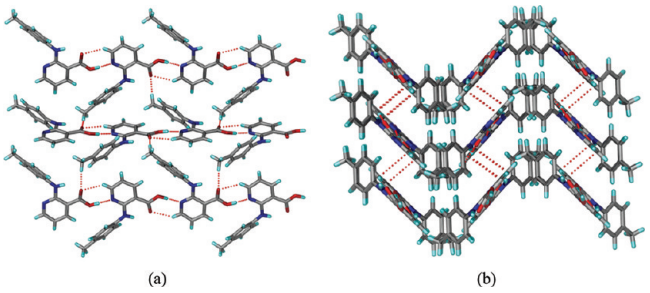

Figure 2. Zigzag sheets of acid−pyridine synthon (a) are connected by $\pi\cdots\pi$ stacking (b) in form II.

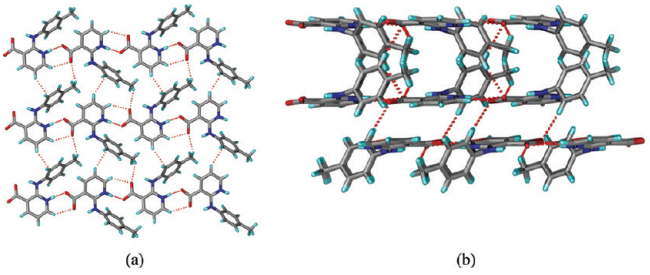

Figure 3. Carboxylate−pyridinium heterosynthon (a) and C−H···O interactions (b) in form III.

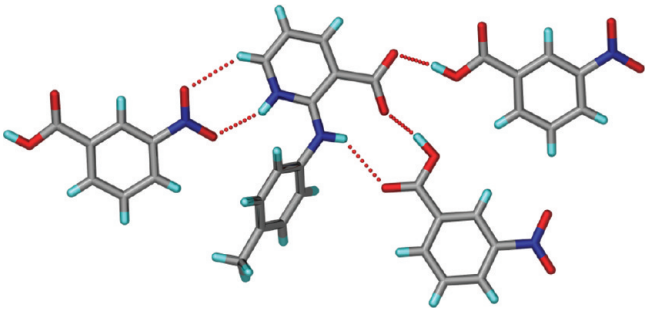

Figure 4. Hydrogen bonding in TNA·2NBA cocrystal, which has a zwitterionic molecule NH^+−TNA−COO^- and two neutral NBA coformers in the crystal structure.

137.0°) is interlinked by C−H···π (C4−H4···C12, 2.85 Å, 146.4°) and C−H···O interactions (C13−H13A···O2, 2.71 Å, 136.9°) in the 100 K data set structure. There are C−H···O interactions (C9−H9···O2, 2.46 Å, 164.0° and C12−H12···O1, 2.52 Å, 172.4°) on either side of the 2D sheets (Figure 3).

The cocrystal of TNA and *m*-nitrobenzoic acid contains one zwitterionic molecule of TNA and two NBA molecules (NH^+−TNA−COO^-·2NBA). However, the normally expected pyridinium−carboxylate synthon of strong N−H^+···O^- hydrogen bond is replaced by pyridinium−nitro group interactions ($N1^+$−H1···O6, 2.17 Å, 152.5°; C5−H5···O5, 2.53 Å, 138.8°). The carboxylic acid donors of two NBA molecules hydrogen bond to the carboxylate acceptor (O3−H3A···O1, 1.66 Å, 170.1°; O8−H8A···O2, 1.63 Å, 170.4°), as shown in Figure 4.

The salt of TNA and *o*-aminopyridine (AP−NH^+·TNA−COO^-) has a classical crystal structure sustained by pyridinium−carboxylate hydrogen bonding (N4−H4A$^+$···O2$^-$, 1.74 Å, 177.3°; N3−H3B···O1$^-$, 1.95 Å, 176.1°) with the AP pyridine

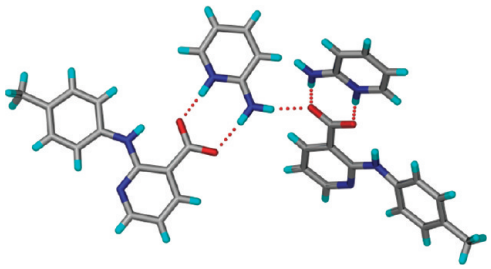

Figure 5. N−H···O synthon in the crystal structure of salt AP−NH^+·TNA−COO^-.

N being protonated and TNA existing as a carboxylate; the TNA pyridine N is free (Figure 5).

The carboxylic acid proton state was verified by the analysis of C−O bond distances, O−C−O bond angles of carboxylic acid/carboxylate group, and C−N−C bond angles of the pyridine ring in the crystal structures (Table 3). The length of the two C−O bond distances in form I (1.30 and 1.23 Å) and form II (1.32 and 1.22 Å) indicate a neutral COOH group, whereas the near equal C−O bond distances in form III (1.26 Å and 1.25 Å) imply a COO^- group. Similarly, O−C−O and C−N−C bond angles argue in favor of a zwitterionic structure in form III but neutral structures of forms I and II. There is a slight difference in the proton state between the crystal structures of form III determined at 100 and 298 K (referred to as LT and RT). The proton is fully located on the pyridine N and the carboxylate group is ionic in the LT crystal structure. The transfer of proton from COOH to pyridine N is slightly less so at RT. There is partial proton occupancy near both O and N atoms in the ORTEP (Figure S1, Supporting Information). This slight drift of the proton from the ionic to the neutral state with an increase in temperature from 100 to 300 K is reflected in the bond distances and angles parameters (Table 3). The difference between the C−O values increases slightly and the C−N−C angle shrinks by 1°.

Comparison of Forms I and III. Forms I and III exhibit 2D isostructural sheets, even though they contain different hydrogen bond synthons (form I, acid−pyridine; form III, pyridinium−carboxylate). Their space group and unit cell parameters are different (Table 1), but their molecular conformations are similar (Figure 6). The main torsion angle is the twist around the diarylamine group listed in Table 4. The calculated X-ray powder diffraction lines from the crystal structures of forms I and III exhibit very close 2θ values (Figure 7). The PXRD pattern of form II is visibly different, as is its molecular packing in the crystal structure. The main structural difference between polymorphs I and III is in the direction of the molecular layers within the identical 2D sheets. If the direction of TNA molecules connected by carboxylic acid−pyridine (in form I) or carboxylate−pyridinium (in form III) running in one direction (right to left) is designated as X and the opposite direction as Y, then adjacent layers contain the motif XYXYXYXY in form I, whereas the sequence is XXYYXXYY in form III (Figure 8). Thus, the difference is more than just a shift of the proton; the sequence arrangement of identical 2D sheets in the third dimension is the major difference between forms I and III. A similar packing difference between the polymorphs of the anti-inflammatory drug nimesulide was noted recently.[16]

In contrast to the crystal structures of related (phenylamino) nicotinic acids reported recently,[11] we neither observed a high Z' crystal structure nor the acid···acid homodimer in TNA

Table 3. C−O Bond Distances and O−C−O and C−N−C Bond Angles in the Crystal Structures of TNA

	bond distances (Å)		angles (deg)	
polymorph	C1−O1	C1−O2	O1−C1−O2	C5−N1−C6
form I at 100 K	1.303(4)	1.217(3)	123.9(3)	119.1(3)
form II at 100 K	1.316(2)	1.223(2)	123.3(1)	118.8(1)
form III at 100 K	1.261(3)	1.249(3)	125.9(2)	122.7(2)
form III at 298 K	1.269(5)	1.242(5)	125.7(3)	121.0(3)
NH^+−TNA−COO^-·2NBA at 298 K	1.245(2)	1.236(2)	125.6(1)	123.8(1)
AP−NH^+·TNA−COO^- at 298 K	1.252(2)	1.266(2)	118.2(2)	118.2(2)

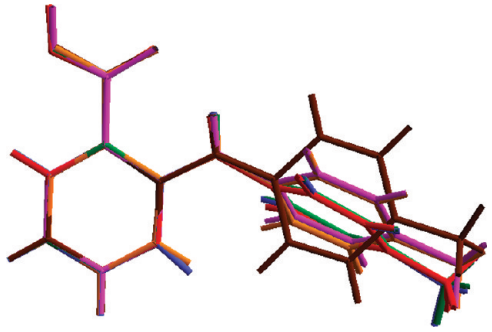

Figure 6. Overlay of all the conformations in TNA crystal structures: TNA form I (red), TNA form II (magenta), TNA form III (100 K) (blue), TNA form III (298 K) (green), NH^+−TNA−COO^-·2NBA (orange), and AP−NH^+·TNA−COO^- (brown).

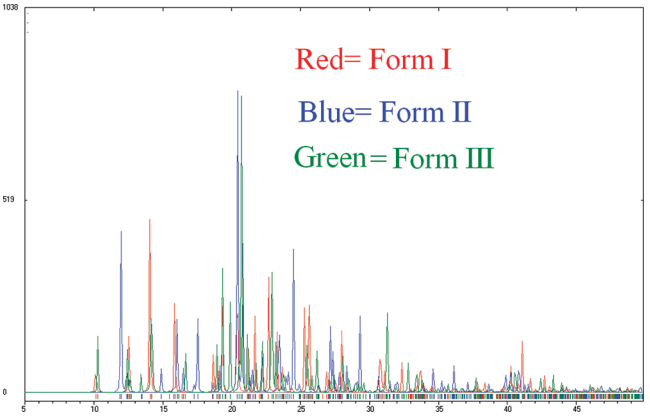

Figure 7. Overlay of calculated PXRD patterns of TNA polymorphs from the crystal structures: form I, red; form II, blue; and form III, green.

Table 4. Torsion Angles for All the Conformations of TNA in Its Crystal Structures

crystal structure	C6−N2−C7−C8 torsion angle (deg)
TNA form I	68.0(4)
TNA form II	55.2(2)
TNA form III (100K)	66.5(3)
TNA form III (298K)	66.8(6)
NH^+−TNA−COO^-·2NBA	55.0(2)
AP−NH^+·TNA−COO^-	11.1(3)

polymorphs. A cocrystal containing acid−base functional groups was part of the fourth Crystal Structure Prediction blind test conducted by the CCDC in 2007.[17] The crystal structure in that case, a 1:1 cocrystal of 2-amino-4-methylpyrimidine and 2-methylbenzoic acid, was correctly predicted by both synthon-based and purely computational approaches.[18] Crystal structures of salts have also been predicted[19] but not of a zwitterionic molecule to our knowledge. Molecular electrostatic potential is yet another tool to map hydrogen bond strengths and preferences. After examining the outcome of crystallization for over a dozen aminopyridines and carboxylic acids, Aakeröy[20] concluded that when the calculated electrostatic charge (MEPS in AM1 package) on the pyridine N is between −220 and −260 kJ/mol, a cocrystal is formed, and when the value is between −275 and −290 kJ/mol, the outcome is a salt. The MEP value for pyridine N in TNA is −268 kJ/mol (calculated in SPARTAN 10,[21] Figure 9), placing this molecule in the gray zone and a difficult to predict case. The fact that both neutral and ionic polymorphs of TNA are observed implies that kinetic factors and experimental conditions could be important in the crystallization of such polymorphs (discussed later).

XPac Analysis. The XPac method[22] is a useful tool to display packing arrangements in crystal structures and to quantify their degree of similarity. XPac analysis of TNA structures I and III produced a 2D supramolecular construct (Figure 10a). The XPac plot (Figure 10b) of δ_p vs δ_a (in degrees) displays the degree of similarity. Both δ_p and δ_a points lie close to the origin, which implies a similarity of the structures being compared. The XPac dissimilarity index X is 3.5%, which gives the similarity of the 2D supramolecular constructs.

Thermal and Spectroscopic Characterization. The three polymorphs of TNA exhibited very close melting endotherms in differential scanning calorimetry (DSC): forms I, II, and III melt at 205, 207, and 204 °C, respectively (Figure 11). No phase transition was detected, suggesting a monotropic relationship among the trimorphs. Even though the melting endotherms are very close, they were reproducible in multiple batches.

The infrared O−H and N−H stretching frequencies of all the three polymorphs of TNA are broad and the carbonyl stretching frequencies are significantly different. The carbonyl stretch for form III (1635 cm^{-1}) is at a lower wavenumber compared to form I (1663 cm^{-1}) and form II (1658.7 cm^{-1}), consistent with the carboxylate group vs carboxylic acid stretching frequency. The pyridine ring shows four skeletal vibrational bands in the 1600−1430 cm^{-1} wavenumber range. The pyridine ring bands are very close in form I (1602, 1579, 1518, 1459 cm^{-1}) and form II (1602, 1578, 1518, 1459 cm^{-1}), but they are different for form III (1604, 1564, 1514 cm^{-1}), and the fourth peak at 1460 cm^{-1} was not observed (see Figure 12 and Table 5). The appearance of a broad O−H stretch in the IR spectrum (centered at 3428 cm^{-1})

dx.doi.org/10.1021/cg200853u |Cryst. Growth Des. 2011, 11, 4594–4605

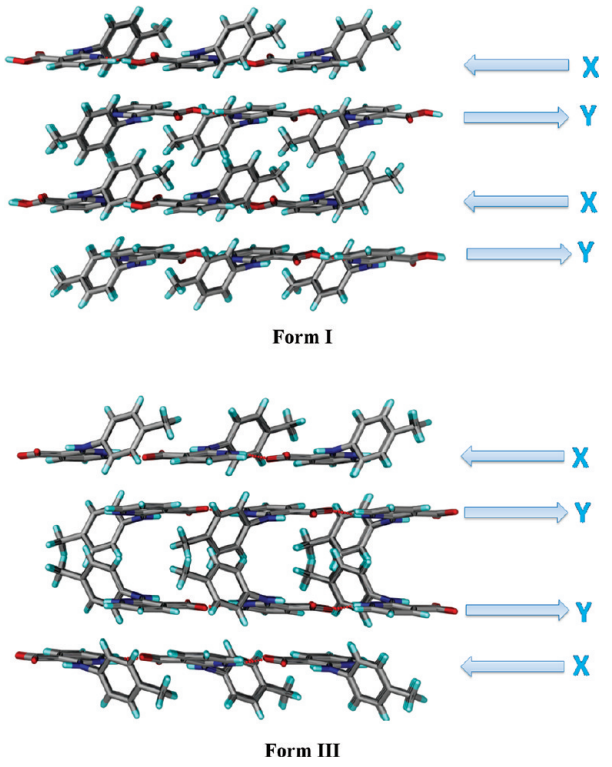

Figure 8. Adjacent layer in the crystal structures of TNA polymorphs. The sequence is XYXYXYXY in form I but XXYYXXYY in form III. Notice that the tolyl methyl groups are oriented in opposite directions in the central portion of form I (XY interlayer region), whereas they are oriented adjacent to each other in form III (YY interlayer region). The other difference is in the hydrogen bonding: neutral O−H···N in form I and ionic $N-H^{+}\cdots O^{-}$ in form III.

indicates partial proton transfer in form III at room temperature, which is consistent with the single crystal X-ray structure analysis at 298 K. The FT-Raman spectra were analyzed for diagnostic peaks (Figure S2 and Table S1, Supporting Information).

Solid-state NMR spectroscopy is a useful technique to differentiate polymorphic structures.[23] ^{15}N and ^{13}C ss-NMR spectra of TNA polymorphs were recorded. There is an upfield shift ∼1 ppm for pyridine N in the ^{15}N ss-NMR spectrum of form III (−146.8 ppm) compared to form I (−147.5 ppm), whereas the chemical shift for form II is at −143.0 ppm. ^{15}N ss-NMR spectra are displayed in Figure 13 and the chemical shift values are listed in Table 6. Normally a large upfield chemical shift is expected as the free pyridine N becomes protonated (about 80−100 ppm).[24] A reason why there is no shift of the ^{15}N nucleus despite a change in the ionization state of the crystal structures of forms I and III is explained by the RT crystal structure of polymorph III. The RT structure of form III depicts an in-between proton situation of neutral and ionic states. The LT structure is clearly zwitterionic. Since ss-NMR spectra were recorded at room temperature, the chemical environment of the pyridine N is more neutral-like than ionic. An IR spectrum of the ss-NMR sample at the end of the measurement confirmed that grinding of the solid for NMR sample preparation had not caused any accidental phase transformation to form I; form III was present after the NMR measurement.

^{13}C ss-NMR spectra of forms I and III exhibit almost identical chemical shift values, since they are 2D isostructural, whereas form II peaks are clearly different (Figure 14 and Table 7).

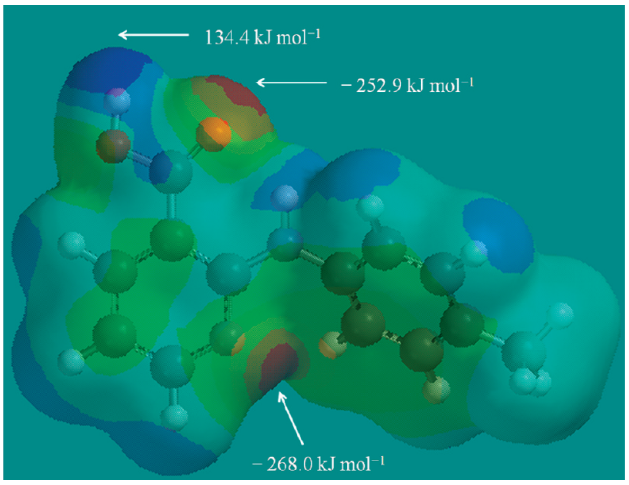

Figure 9. Electrostatic surface potential (ESP) calculated for TNA molecule in Spartan (AM1). The molecular structure was constructed in GaussView 3.0 and optimized in Spartan 10.

Hirshfeld Plots. Hirshfeld 2D fingerprint plots[25] of the three polymorphs highlight the differences in their intermolecular contacts (Figure 15). The sharp spikes for the O···H interactions in form III at $d_e = d_i \approx 1.0$ are due to the short $N-H^{+}\cdots O^{-}$ hydrogen bond, whereas these protrusions are absent in plots of forms I and II. The complementary situation in forms I and II of short N···H contacts due to a strong O−H···N hydrogen bond is represented by the sharp spikes at $d_e = d_i \approx 1.0$, whereas they are absent for form III. The C−H···O hydrogen bonds occur at longer distance of $d_e = d_i \approx 1.4$. These plots are yet another manifestation of the neutral O−H···N hydrogen bond in polymorphs I and II and ionic $N-H^{+}\cdots O^{-}$ hydrogen bond in form III. The π-stacking of linear hydrogen-bonded tapes in structures of forms I and III ($d_e = d_i \approx 2.5$) is less dense in form II. The major intermolecular interactions in TNA polymorphs are depicted in Figure 16. The contribution from N···H interactions to the Hirshfeld surface is higher in form I (7.4%) and form II (8.6%) than that in form III (2.3%), whereas the contribution from O···H interactions follows the opposite trend (form III 20.6%, form II 14.6%, form I 14.4%).

What is the Role of Pyridine Coformers in Giving a Zwitterionic Structure of TNA? Our observation that zwitterionic form III could be obtained only in the presence of pyridine-type coformers is not an isolated occurrence. Several cases are reported in the literature[23d,26] wherein a new polymorph was discovered during attempted cocrystallization. Even so, this is the first instance of a zwitterionic polymorph being crystallized in the presence of coformer additives. Despite the frequent occurrence of such reports, a plausible explanation for this phenomenon is still elusive. The crystallization of a salt structure with *o*-aminopyridine wherein TNA exists as a carboxylate anion and AP is a pyridinium cation could offer an explanation, at least in this instance. The similarity of the pK_a of pyridine base, whether the moiety is present in TNA or AP, suggested that there could be a dynamic equilibrium between several species in solution (Scheme 4), a few neutral ones and others ionic. Depending on the solvent of cocrystallization, temperature, coformer, additive, supersaturation, etc., the concentration of the neutral adduct, salt, and zwitterion will vary depending on the solubility of that species in the crystallization medium. The species that is

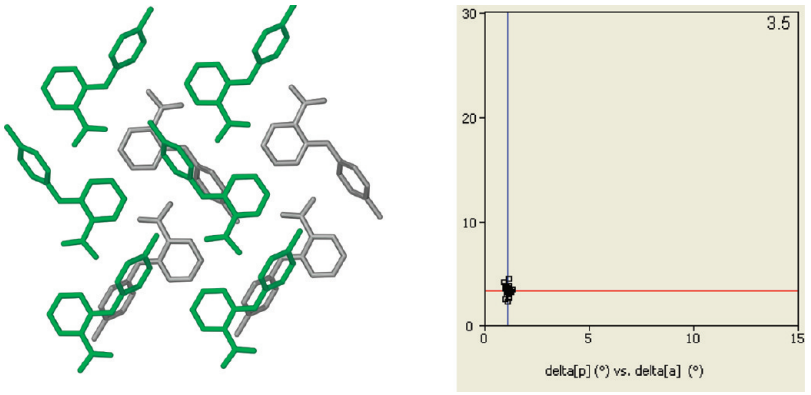

Figure 10. (a) 2D supramolecular construct identified by XPac analysis of TNA forms I and III. Molecules in different layers are shaded differently. (b) Plot of interplanar angular deviation (δ_p, *x*-axis) vs angular deviation (δ_a, *y*-axis) in degrees.

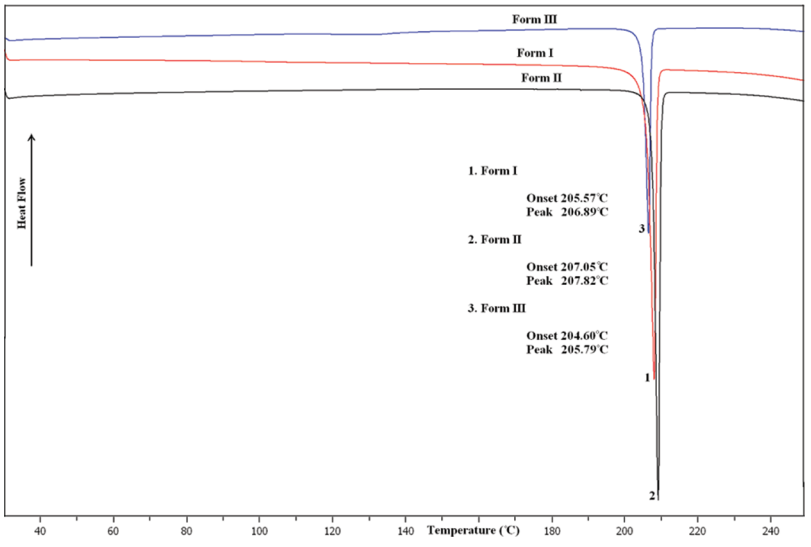

Figure 11. DSC thermograms of form I (red), form II (black), and form III (blue) of TNA. The endotherms are sharp and the T_{peak} values are barely 1 °C apart.

the most supersaturated in a given solvent will precipitate first and the product of such a cocrystallization experiment will strongly depend upon the supersaturation conditions and, consequently, on crystallization parameters such as solvent, temperature, concentration, rate of cooling, etc. Because solvent selection in cocrystallization experiments is usually a trial-and-error process, by testing the solubility of the components in different solvents and mixtures, the outcome is often a serendipitous result when a new polymorph of one of the components is discovered. A possible pathway to zwitterionic polymorph III under cocrystallization conditions is depicted in Scheme 4. Could a general recipe to obtain the zwitterionic polymorphs of acid−base compounds be optimized by using coformers whose acidic/basic functional groups are of a similar pK_a to that of the molecule? Those solvents in which the ionic form is likely to supersaturate should be preferable for crystallization. The selective crystallization of zwitterionic polymorphs for acid−base drugs will have an immediate application for solubility improvement. Experiments are currently under way to establish a general protocol along these lines. The design parameters will best operate in the gray zone of ΔpK_a between 0 and 3 when there is dynamic proton equilibrium between the acid and the base. When $\Delta pK_a < 0$ or > 3, the outcome is a predictable neutral cocrystal or ionic salt.

CONCLUSIONS

TNA is as the third example of a polymorphic molecule exhibiting neutral and zwitterionic crystal structures with 3D coordinates determined after clonixin and norfloxacin. Anthranilic acid and torasemide are in a different category in that both neutral and zwitterionic molecules are present in the same crystal structure. Crystallization of the zwitterionic polymorph III of TNA was observed only in the presence of pyridine coformers, more often with *o*-bromo-*m*-hydroxypyridine. Interestingly, a zwitterionic two-component structure of TNA cocrystallized with *m*-nitrobenzoic acid and a salt with *o*-aminopyridine. These preliminary observations suggest a role for the coformer in directing the crystallization toward a polymorph, a cocrystal, or a salt. Even though zwitterionic structures of acid−base organic molecules are known, the occurrence of both neutral and zwitterionic polymorphs for the same compound is as such rare.

dx.doi.org/10.1021/cg200853u |*Cryst. Growth Des.* 2011, 11, 4594–4605

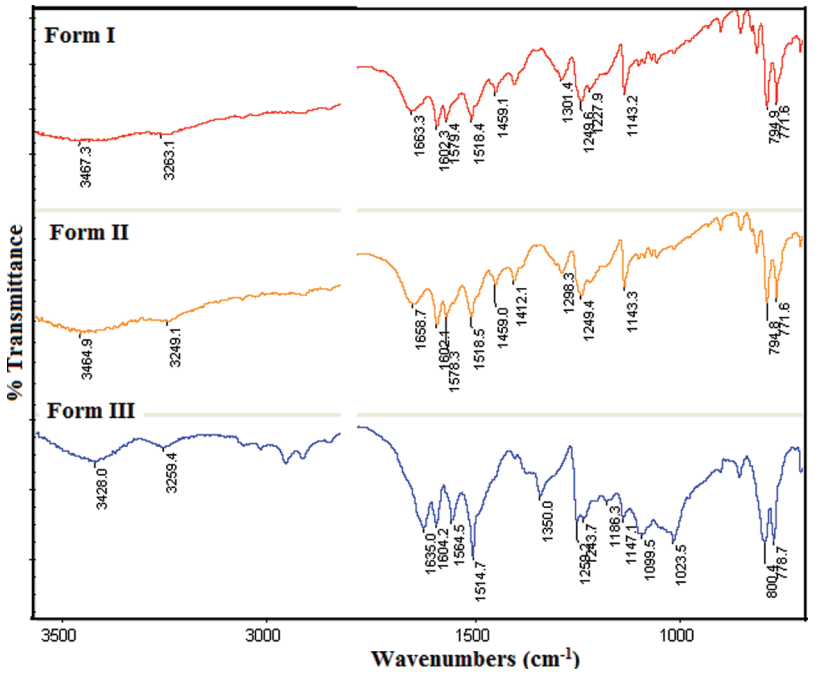

Figure 12. FT-IR comparison of TNA forms I−III.

Table 5. FT-IR (KBr pallet) Spectral Bands of TNA Polymorphs

polymorph	O−H stretch (br) (cm^{-1})	N−H stretch (br) (cm^{-1})	C═O stretch (cm^{-1})	pyridine ring stretch (cm^{-1})
form I	3467.3	3263.1	1663.3	1602, 1579.4, 1518, 1459
form II	3464.9	3249.1	1658.7	1602, 1578, 1518, 1459
form III	3428.0	3259.4	1635.0	1604, 1564, 1514

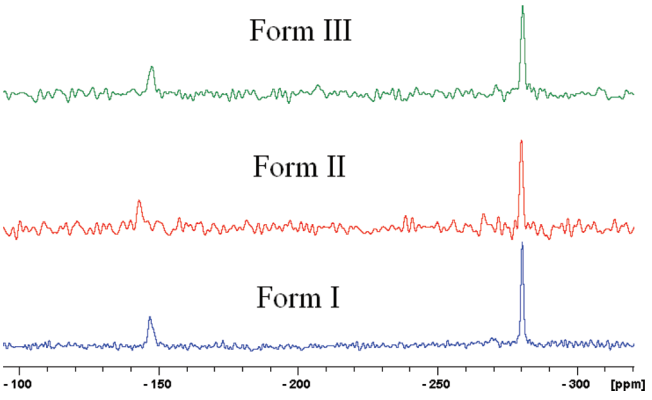

Figure 13. ^{15}N ss-NMR for TNA forms I−III.

Studies are ongoing to optimize the crystallization of zwitterionic polymorphs for (aminophenyl)nicotinic acids.

EXPERIMENTAL SECTION

General. All solvents, reagents, and coformers were purchased from commercial sources and used without further purification.

Table 6. ^{15}N ss-NMR Chemical Shifts (δ, ppm) of TNA Polymorphs

polymorph	pyridine N	2° amine N
form I	−147.6	−280.5
form II	−143.0	−280.0
form III	−146.8	−280.3

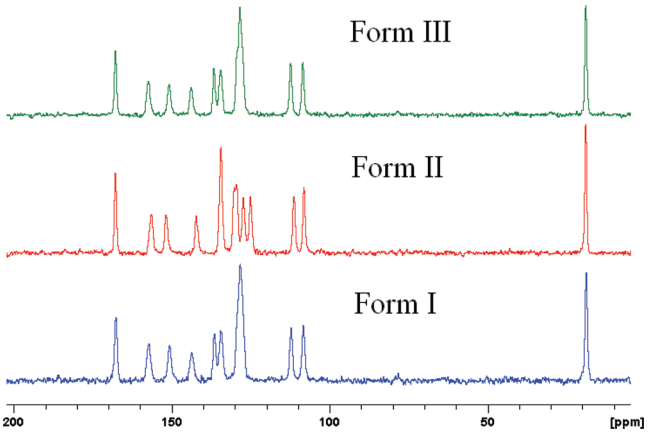

Figure 14. ^{13}C ss-NMR of TNA forms I−III.

Synthesis. TNA was synthesized[27] by refluxing *o*-chloronicotinic acid (315.3 mg, 2 mmol), *p*-toluidine (214.3 mg, 2 mmol), *p*-toluenesulfonic acid (95.0 mg, 0.5 mmol), and few drops of pyridine in water and acetone solution (1:4, 10 mL) at 70 °C overnight (about 8 h) (Scheme 5). The precipitated product was filtered and purified by crystallization from acetone to obtain pure 2-(*p*-tolylamino)nicotinic acid (TNA), which was characterized by ^{1}H NMR, ^{13}C NMR, and IR. ^{1}H NMR ($CDCl_3$, 400 MHz): δ 9.99 (s, 1H), 8.40 (d, J = 8 Hz, 1H), 8.31 (d, J = 8 Hz, 1H), 7.52 (d, J = 8 Hz, 1H), 7.19 (d, J = 8 Hz, 2H), 6.72 (d,

dx.doi.org/10.1021/cg200853u |*Cryst. Growth Des.* 2011, 11, 4594–4605

J = 8 Hz, 2H), 2.33 (s, 3H). ^{13}C NMR ($CDCl_3$, 100 MHz): δ 171.35, 156.68, 153.50, 141.53, 136.39, 133.46, 129.51, 122.25, 113.05, 20.90. IR (KBr, cm^{-1}): 3441.2, 3254.2, 3068.4, 1669.3, 1602.2, 1579.4, 1517.6, 1459.3, 1412.6, 1248.9, 1143.3, 795.5. Mp: 205−207 °C.

CSD Search. A search of the CSD (version 5.31, November 2010; May 2011 update)[4] was performed using the following functional groups as search criteria (Table 8), all organic compounds with the word "form", "polymorph", "modification", and "phase" in the qualifier, excluding the entries for which 3D coordinates are not available. These searches resulted in only four zwitterionic and neutral polymorphic sets for single component organic molecules with solved X-ray crystal structures.

X-ray Crystallography. X-ray reflections for TNA forms I and III (LT data) and AP−NH^+·TNA−COO^- salt were collected on a Bruker SMART APEX CCD diffractometer equipped with a graphite monochromator and Mo Kα fine-focus sealed tube (λ = 0.710 73 Å). Data integration was done using SAINT.[28] Intensities for absorption were corrected using SADABS.[29] Structure solution and refinement were carried out using Bruker SHELX-TL.[30] X-ray reflections for TNA forms II and III (RT data) and N−H^+−TNA−COO^-·2NBA were collected on an Oxford Xcalibur Gemini Eos CCD diffractometer using Mo Kα, radiation. Data reduction was performed using CrysAlisPro (version 1.171.33.55). OLEX2-1.0[31] and SHELX-TL 97 were used to solve and refine the data. All non-hydrogen atoms were refined anisotropically,

Table 7. ^{13}C ss-NMR Chemical Shifts (δ, ppm) of TNA Polymorphs

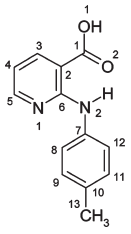

numbering in the above structure	form I	form II	form III
C13	18.6	18.7	18.7
C2	108.2	108.0	108.3
C4	112.0	111.1	112.1
C8, C12	128.1 (merged)	124.9	128.2 (merged)
C10		127.1	
C9, C11	134.3	129.3	134.3
C3	136.2	134.2	136.4
C7	143.5	142.0	143.6
C5	150.4	151.6	150.6
C6	157.1	156.2	157.2
C1	167.5	167.6	167.6

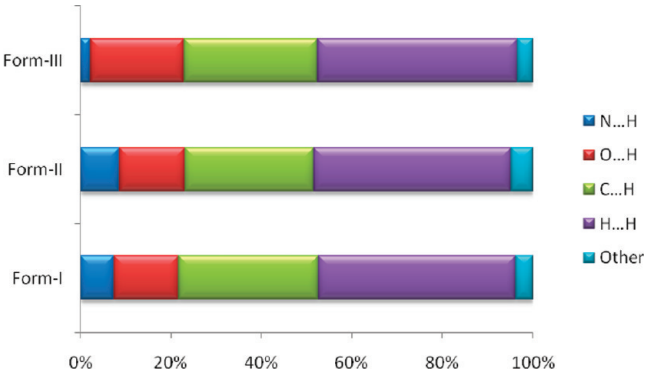

Figure 16. Contribution from major interactions to the Hirshfeld surface.

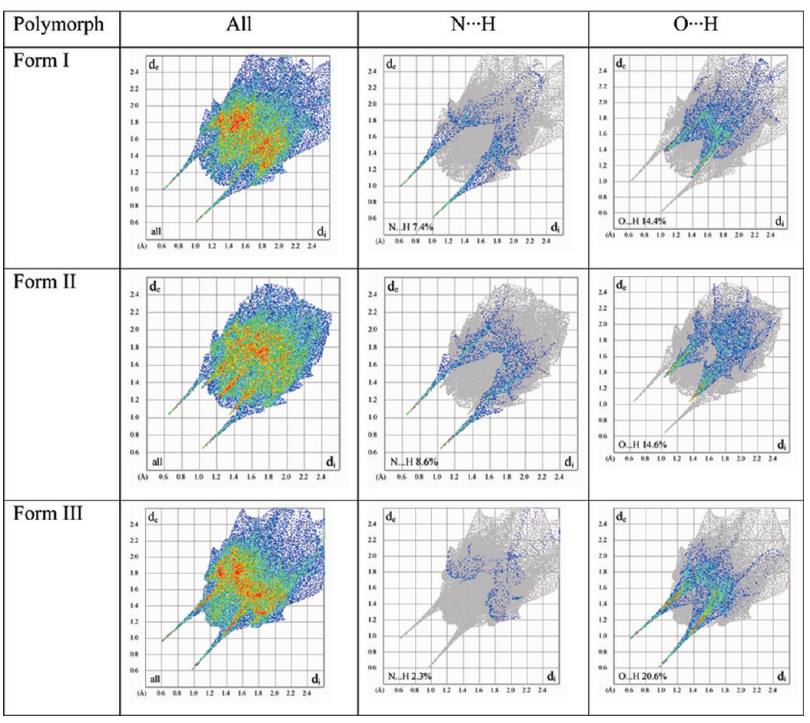

Figure 15. 2D Hirshfeld fingerprint plot for three TNA polymorphs, forms I−III. Note that the O···H and N···H plots are different for polymorphs I and III. The sharp blue spikes occur in the N···H plot for form I but in the O···H plot for form III.

dx.doi.org/10.1021/cg200853u |*Cryst. Growth Des.* 2011, 11, 4594–4605

Scheme 4. Equilibrium Between Soluble and Supersaturated Components, TNA and AP, in CH_3CN Solvent[a]

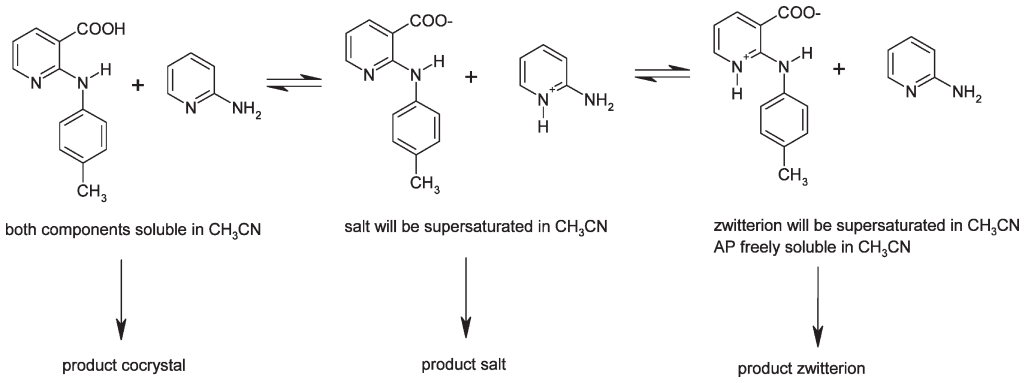

[a] This kind of equilibrium situation will most probably be present in solution when $0 < \Delta pK_a < 3$.

Scheme 5. Synthesis of 2(*p*-Tolylamino)nicotinic Acid (TNA)

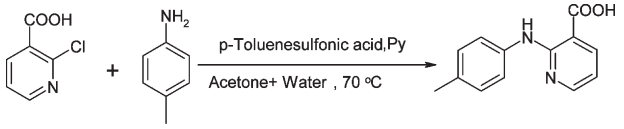

Table 8. Functional Groups Used To Search the CSD and the Number of Hits Retrieved

substructure	no. of hits	substructures	no. of hits
N and COOH	411	NH^+ and COO^-	407
N and SO_3H	10	NH^+ and SO_3^-	118
N and PO_4H	31	NH^+ and PO_4^-	31
N and OH	1276	NH^+ and O^-	807
N and NC(=O)N	166	NH^+ and $(NH^-)C(=O)N$	3

and C−H hydrogens were fixed. N−H and O−H hydrogens were located from difference electron density maps and C−H hydrogens were fixed. Packing diagrams were prepared in X-Seed.[32] Crystallographic .cif files (CCDC Nos. 833063−833068) are available at www.ccdc.cam.ac.uk/data_request/cif or as part of the Supporting Information.

Vibrational Spectroscopy. Nicolet 6700 FT-IR spectrometer with an NXR FT-Raman module was used to record IR and Raman spectra. IR spectra were recorded on samples dispersed in KBr pellets. Raman spectra were recorded on solid samples contained in standard NMR diameter tubes or on compressed samples contained in a gold-coated sample holder.

ss-NMR Spectroscopy. Solid-state NMR spectra were recorded on a Bruker Avance spectrometer at 400 MHz. ss-NMR spectra were recorded on a Bruker 4 mm double-resonance CP-MAS probe in zirconia rotors at 5.0 kHz spin rate with a cross-polarization contact time of 2.5 ms and a recycle delay of 8 s. ^{13}C CP-MAS spectra recorded at 100 MHz were referenced to the methylene carbon of glycine and then the chemical shifts were recalculated to the TMS scale ($\delta_{glycine}$ = 43.3 ppm). Likewise, ^{15}N CP-MAS spectra recorded at 40 MHz were referenced to glycine N and then the chemical shifts were recalculated to nitromethane ($\delta_{glycine}$ = −347.6 ppm).

Thermal Analysis. DSC was performed on Mettler Toledo DSC 822e module. Samples were placed in crimped but vented aluminum sample pans. The typical sample size was 3−4 mg, and the temperature range was 30−250 °C at heating rate of 5 °C/min. Samples were purged by a stream of dry nitrogen flowing at 150 mL/min.

■ ASSOCIATED CONTENT

Supporting Information. Additional information as noted in the text. This material is available free of charge via the Internet at http://pubs.acs.org.

■ AUTHOR INFORMATION

Corresponding Author
*E-mail: ashwini.nangia@gmail.com.

■ ACKNOWLEDGMENT

This research was funded by the DST (SR/S1/OC-67/2006), CSIR (01-2410/10/EMR-II), a JC Bose Fellowship (SR/S2/JCB-06/2009), and UGC (PURSE grant). N.K.N. and S.S.K. thank the UGC and CSIR for fellowships.

■ REFERENCES

(1) Lehninger, A. L.; Nelson, D. L.; Cox, M. M. *Principles of Biochemistry*, 2nd ed.; Worth Publishers; New York, 1993; pp 81−83.

(2) (a) Tam, K. Y.; Avdeef, A.; Tsinman, O.; Sun, N. *J. Med. Chem.* **2010**, *53*, 392. (b) Ranney, D. F. *Biochem. Pharmacol.* **2000**, *59*, 105. (c) Marcus, S.; Bernstein, M.; Ziv, G.; Glickman, A.; Gipps, M. *Vet. Res. Commun.* **1994**, *18*, 331.

(3) Tong, W.-Q. In *Developing Solid Oral Dosage Forms. Pharmaceutical Theory and Practice*; Qiu, Y., Chen, Y., Zhang, G. G. Z., Eds.; Academic Press: New York, 2009; pp 75−86.

(4) Cambridge Structural Database, ver. 5.31, ConQuest 1.13, November 2010 release, Cambridge Crystallographic Data Center; www.ccdc.cam.ac.uk.

(5) Takasuka, M.; Nakai, H.; Shiro, M. *J. Chem. Soc., Perkin Trans. 2* **1982**, 1061(BIXGIY01, BIXGIY02, BIXGIY03, BIXGIY04).

(6) (a) Basavoju, S.; Bostrom, D.; Velaga, S. P. *Cryst. Growth Des.* **2006**, *6*, 2699 (VETVOG). (b) Barbas, R.; Prohens, R.; Puigjaner, C. *J. Thermal Anal. Calorim.* **2007**, *89*, 687 (VETVOG01).

(7) (a) Khan, M. Y.; Srivastava, P. *Indian J. Pure Appl. Phys.* **1968**, *6*, 166 (AMBACO). (b) Brown, C. J. *Proc. R. Soc. London, Ser. A* **1968**, *302*, 185 (AMBACO01, AMBACO02). (c) Boone, C. D. G.; Derissen, J. L.; Schoone, J. C. *Acta Crystallogr.* **1977**, *B33*, 3205(AMBACO03). (d) Murti, K. *Indian J. Phys.* **1957**, *31*, 611(AMBACO04). (e) Hardy, G. E.; Kaska, W. C.; Chandra, B. P.; Zink, J. I. *J. Am. Chem. Soc.* **1981**,

103, 1074 (AMBACO05, AMBACO06). (f) Brown, C. J.; Ehrenberg, M. *Acta Crystallogr.* **1985**, *C41*, 441 (AMBACO07). (g) Takazawa, H.; Ohba, S.; Saito, Y. *Acta Crystallogr.* **1986**, *C42*, 1880 (AMBACO08). (h) Lu, T. H.; Chattopadhyay, P.; Liao, F. L.; Lo, J. M. *Anal. Sci.* **2001**, *17*, 905 (AMBACO09).

(8) (a) Dupont, L.; Dive, G. *Bull. Soc. R. Sci. Liege* **1982**, *51*, 248 (TORESEM02). (b) Bartolucci, G.; Bruni, B.; Coran, S. A.; Vaira, M. D. *Acta Crystallogr.* **2009**, *E65*, o972 (TORESEM04).

(9) Thomas, M. J.; Thomas, J. A. In *Modern Pharmacology with Clinical Applications*, 5th ed.; Craig, C. R., Stitzel, R. E., Eds.; Little Brown & Co.: Boston, 1997.

(10) (a) Lee, E. H; Byrn, S. R.; Carvajal, M. T. *Pharm. Res.* **2006**, *23*, 2375. (b) McConnell, J. F.; Company, F. Z. *Cryst. Struct. Commun.* **1976**, *5*, 861. (c) Fang, L.; Numajiri, S.; Kobayashi, D.; Ueda, H.; Nakayama, K.; Miyamae, H.; Morimoto, Y. *J. Pharm. Sci.* **2004**, *93*, 144. (d) Andersen, K. V; Larsen, S.; Alhede, B.; Gelting, N.; Buchardt, O. J. *Chem. Soc., Perkin Trans. 2* **1989**, 1443. (e) Lopez-Mejias, V.; Kampf, J. W.; Matzger, A. J. *J. Am. Chem. Soc.* **2009**, *131*, 4554. (f) Surov, A. O.; Szterner, P.; Zielenkiewicz, W.; Perlovich, G. L. *J. Pharm. Biomed. Anal.* **2009**, *50*, 831. (g) McConnell, J. F. *Cryst. Struct. Commun.* **1973**, *2*, 459. (h) Murthy, M. H. K.; Bhat, T. N.; Vijayan, M. *Acta Crystallogr.* **1982**, *B38*, 315. (i) Lee, E. H.; Boerrigter, S. X. M; Rumondor, A. C. F.; Chamarthy, S. P.; Byrn, S. R. *Cryst. Growth Des.* **2008**, *8*, 91. (j) Eun Hee Lee, E. H.; Boerrigter, S. X. M.; Byrn, S. R. *Cryst. Growth Des.* **2010**, *10*, 518. (k) Moser, P.; Sallmann, A.; Wiesenberg, I. *J. Med. Chem.* **1990**, *33*, 2358. (m) Demertzi, D. K.; Mentzafos, D.; Terzis, A. *Polyhedron* **1993**, *12*, 1361. (n) Castellari, C.; Ottani, S. *Acta Crystallogr.* **1997**, *C53*, 794. (o) Jaiboon, N.; Yos-In, K.; Ruangchaithaweesuk, S.; Chaichit, N.; Thutivoranath, R.; Siritaedmukul, K.; Hannongbua, S. *Anal. Sci.* **2001**, *17*, 1465. (p) Muangsin, N.; Prajuabsook, M.; Chimsook, P.; Chantarasiri, N.; Siraleartmukul, K.; Chaichit, N.; Hannongbua, S. *J. Appl. Crystallogr.* **2004**, *37*, 288. (q) Perlovich, G. L.; Surov, A. O.; Hansen, L. K.; Brandl, A. B. *J. Pharm. Sci.* **2007**, *96*, 1031. (r) Surov, A. O.; Terekhova, I. V.; Bauer-Brandl, A.; Perlovich, G. L. *Cryst. Growth Des.* **2009**, *9*, 3265.

(11) (a) Long., S.; Parkin, S.; Siegler, M. A.; Cammers, A.; Li, T. *Cryst. Growth Des.* **2008**, *8*, 4006. (b) Long, S.; Li, T. *Cryst. Growth Des.* **2009**, *9*, 4993. (c) Long, S.; Li, T. *Cryst. Growth Des.* **2010**, *10*, 2465. (d) Long, S.; Parkin, S.; Siegler, M.; Brock, C. P.; Cammers, A.; Li, T. *Cryst. Growth Des.* **2008**, *8*, 3137. (e) Long, S.; Siegler, M. A.; Mattei, A.; Li, T. *Cryst. Growth Des.* **2011**, *11*, 414.

(12) Sarma, B.; Nath, N. K.; Bhogala, B. R.; Nangia, A. *Cryst. Growth Des.* **2009**, *9*, 1546.

(13) (a) Johnson, S. L.; Rumon, K. A. *J. Phys. Chem.* **1965**, *69*, 74. (b) Childs, S. L.; Stahly, G. P.; Park, A. *Mol. Pharmaceutics* **2007**, *4*, 323. (c) Sarma, B.; Thakuria, R.; Nath, N. K.; Nangia, A. *CrystEngComm* **2011**, *13*, 3232.

(14) (a) Lide, D. R. *CRC Handbook of Chemistry & Physics*, 86th ed.; CRC Press: Boca Raton, FL, 2004; pp 42−51, Chapter 8. (b) Linnell, R. H. *J. Org. Chem.* **1960**, *25*, 290.

(15) Nangia, A. *Acc. Chem. Res.* **2008**, *41*, 595.

(16) Sanphui, P.; Sarma, B.; Nangia, A. *J. Pharm. Sci.* **2011**, *100*, 2287.

(17) Day, G. M.; Cooper, T. G.; Cruz-Cabeza, A. J.; Hejczyk, K. E.; Ammon, H. L.; Boerrigter, S. X. M.; Tan, J. S.; Della Valle, R. G.; Venuti, E.; Jose, J.; Gadre, S. R.; Desiraju, G. R.; Thakur, T. S.; van Eijck, B. P.; Facelli, J. C.; Bazterra, V. E.; Ferraro, M. B.; Hofmann, D. W. M.; Neumann, M. A.; Leusen, F. J. J.; Kendrick, J.; Price, S. L.; Misquitta, A. J.; Karamertzanis, P. G.; Welch, G. W. A.; Scheraga, H. A.; Arnautova, Y. A.; Schmidt, M. U.; van de Streek, J.; Wolf, A. K.; Schweizer, B. *Acta Crystallogr.* **2009**, *B65*, 107.

(18) (a) Neumann, M. A.; Leusen, F. J. J.; Kendrick, J. *Angew. Chem., Int. Ed.* **2008**, *47*, 2427. (b) Thakur, T. S.; Desiraju, G. R. *Cryst. Growth Des.* **2008**, *8*, 4031.

(19) (a) Leusen, F. J. J. *Cryst. Growth Des.* **2003**, *3*, 189. (b) Karamertzanis, P. G.; Price, S. L. *J. Phys. Chem. B* **2005**, *109*, 17134.

(20) Aakeröy, C. B.; Rajbanshi, A.; Li, Z. J.; Desper, J. *CrystEngComm* **2010**, *12*, 423.

(21) *SPARTAN 10, Full Range of Computational Chemistry Software*; Wavefunction Inc.; www.wavefun.com.

(22) (a) Gelbrich, T.; Hursthouse, M. B. *CrystEngComm* **2005**, *7*, 324. (b) Gelbrich, T.; Hursthouse, M. B. *CrystEngComm* **2006**, *8*, 448. (c) Gelbrich, T.; Hughes, D. S.; Hursthouse, M. B.; Threlfall, T. L. *CrystEngComm* **2008**, *10*, 1328. (d) Fabbiani, F. P. A.; Dittrich, B.; Florence, A. J.; Gelbrich, T.; Hursthouse, M. B.; Kuhs, W. F.; Shankland, N.; Sowa, H. *CrystEngComm* **2009**, *11*, 1396.

(23) (a) Bugay, D. E. *Pharm. Res.* **1993**, *10*, 317. (b) Heider, E. M.; Harperb, J. K.; Grant, D. M. *Phys. Chem. Chem. Phys.* **2007**, *9*, 6083. (c) Vickery, R. D.; Nemeth, G. A.; Maurin, M. B. *J. Pharm. Biomed. Anal.* **2002**, *30*, 125. (d) Sanphui, P.; Goud, N. R.; Khandavilli, U. B. R.; Bhanothb, S.; Nangia, A. *Chem. Commun.* **2011**, 5013.

(24) (a) Lorente, P.; Shenderovich, I. G.; Golubev, N. S.; Denisov, G. S.; Buntkowsky, G.; Limbach, H. H. *Magn. Reson. Chem.* **2001**, *39*, S18. (b) Li, Z. J.; Abramov, Y.; Bordner, J.; Leonard, J.; Medek, A.; Trask, A. V. *J. Am. Chem. Soc.* **2006**, *128*, 8199.

(25) (a) Spackman, M. A.; Jayatilaka, D. *CrystEngComm* **2009**, *11*, 19. (b) McKinnon, J. J.; Jayatilaka, D.; Spackman, M. A. *Chem. Commun.* **2007**, 3814.

(26) (a) Nath, N. K.; Nangia, A. *CrystEngComm* **2011**, *13*, 47. (b) Day, G. M.; Trask, A. V.; Motherwell, W. D. S.; Jones, W. *Chem. Commun.* **2006**, 54. (c) Rafilovich, M.; Bernstein, J. *J. Am. Chem. Soc.* **2006**, *128*, 12185. (d) Vishweshwar, P.; McMahon, J. A.; Oliveira, M.; Peterson, M. L.; Zaworotko, M. J. *J. Am. Chem. Soc.* **2005**, *127*, 16802. (e) Bond, A. D.; Solanko, K. A.; Parsons, S.; Redder, S.; Boese, R. *CrystEngComm* **2011**, *13*, 399. (f) Wenger, M.; Bernstein, J. *Mol. Pharmaceutics* **2007**, *4*, 355. (g) Lou, B.; Boström, D.; Velaga, S. P. *Cryst. Growth Des.* **2009**, *9*, 1254. (h) Mei, X.; Wolf, C. *Cryst. Growth Des.* **2004**, *4*, 1099. (i) Thomas, L. H.; Wales, C.; Zhao, L.; Wilson, C. C. *Crystal Growth Des.* **2011**, *11*, 1450. (j) Losev, E. A.; Mikhailenko, M. A.; Boldyreva, E. V. *Proc. RAS, Ser. Phys. Chem.* **2011**, *439* (6), 1.

(27) Ting, P. C.; Kaminski, J. J.; Sherlock, M. H.; Tom, W. C.; Lee, J. F.; Bryant, R. W.; Watnick, A. S.; McPhail, A. T. *J. Med. Chem.* **1990**, *33*, 2697.

(28) *SAINT-Plus, version 6.45*; Bruker AXS Inc., Madison, WI, 2003.

(29) Sheldrick, G. M. *SADABS, Program for Empirical Absorption Correction of Area Detector Data*; University of Göttingen, Germany, 1997.

(30) (a) *SMART* (Version 5.625) and *SHELX-TL* (Version 6.12); Bruker AXS Inc., Madison, WI, 2000. (b) Sheldrick, G. M. *SHELXS-97 and SHELXL-97*; University of Göttingen, Germany, 1997.

(31) Dolomanov, O. V.; Blake, A. J.; Champness, N. R.; Schröder, M. *J. Appl. Crystallogr.* **2003**, *36*, 1283.

(32) Barbour, L. J. *X-Seed, Graphical Interface to SHELX-97 and POV-Ray*; University of Missouri—Columbia, 1999.